Angular reconstruction of a lead scintillating-fiber sandwiched electromagnetic calorimeter[*]

LI Zu-Hao(李祖豪)[1)]   XU Wei-Wei(许伟伟)   WANG Ling-Yu(王玲玉)   ZHANG Cheng(张诚)

TANG Zhi-Cheng(唐志成)   YAN Qi(严琪)   YANG Min(杨民)   LÜ Yu-Sheng(吕雨生)

CHEN Guo-Ming(陈国明)   CHEN He-Sheng(陈和生)

Institute of High Energy Physics, Chinese Academy of Sciences, Beijing 100049, China

Abstract: The Neighbor Cell Deposited Energy Ratio (NCDER) is a new method that is proposed to reconstruct incidence position in a single layer for a 3-dimensional imaging electromagnetic calorimeter (ECAL). This method was applied to reconstruct the ECAL test beam data for the Alpha Magnetic Spectrometer-02 (AMS-02). The results show that this method can achieve an angular resolution of $7.36\pm0.08°/\sqrt{E}\oplus0.28\pm0.02°$ in the determination of the photon's direction, which is much more precise than that obtained with the commonly-adopted Center of Gravity (COG) method ($8.4\pm0.1°/\sqrt{E}\oplus0.8\pm0.3°$). Furthermore, since it uses only the properties of electromagnetic showers, this new method could also be used for other type of fine grain sampling calorimeters.

Key words: electromagnetic calorimeter, angular resolution, lateral fit, Neighbor Cell Deposited Energy Ratio

PACS: 29.40.V.J   **DOI:** 10.1088/1674-1137/38/5/056203

1　Introduction

The Alpha Magnetic Spectrometer-02 (AMS-02) is a particle physics detector that is designed to search for antimatter and dark matter, as well as to accurately measure cosmic ray spectra in space [1]. It was installed on the International Space Station (ISS) on 19th May, 2011 and will record data from cosmic rays for 10 to 20 years. The Electromagnetic Calorimeter (ECAL) of the AMS-02 is a fine-grained lead scintillating-fiber sampling calorimeter which allows for precise, 3-dimensional (3D) imaging of the longitudinal and lateral shower development. The system provides a high electron/hadron discrimination, as well as good energy and angular resolution [2, 3]. The structure of the ECAL and the test beam setup are briefly described in Section 2.

A new method, named Neighbor Cell Deposited Energy Ratio (NCDER) , was used to reconstruct the incidence position in each layer and is compared to two alternative methods, Lateral Fit (LF) and Center Of Gravity (COG), the latter being the most frequently used method. The comparison shows that the NCDER and the LF methods are more precise than the COG method, and the NCDER method is more efficient than the LF method (Section 5).

2　AMS-02 ECAL and test beam

The AMS-02 ECAL is a 3D imaging calorimeter that consists of a pancake composed from 9 super-layer, giving an active area of 648 mm×648 mm and a thickness of 166.5 mm. Each super-layer is 18.5 mm thick and made of 11 grooved, 1 mm thick lead foils interleaved with layers of 1 mm diameter scintillating fibers, glued together with epoxy resin. The detector imaging capability is obtained by stacking super-layers with fibers alternatively parallel to the x-axis (5 layers) and y-axis (4 layers) (Fig. 1(a)). Each super-layer is read out by 36 Photo Multiplier Tubes (PMTs), arranged alternately on the two opposite ends. Fibers are read out, on one end only, by four anode Hamamatsu PMTs. Each anode covers an active area of 9 mm×9 mm, corresponding to 35 fibers, defined as a cell (Fig. 1(b)), the minimum detection unit, which corresponds about 1 radiation length and 0.5 Moliere Radius ($R_{\rm M}$). In total, the ECAL consists of 18 layers, measuring 10 layers in the y direction and 8 layers in the x direction [2, 3].

The flight model of the ECAL was successfully tested and calibrated on the H4 beam line of the Super Proton Synchrotron (SPS) at CERN in July 2007. A schematic diagram of the test beam setup is shown in Fig. 2. The

ECAL flight model was mounted on a rotating table that can move along the x and y axes, and which can rotate around the z axis. Events were triggered by four crossed plastic scintillating counters in coincidence. Three silicon tracker ladders were installed in front of the ECAL, which provided accurate information on the beam incident position. Data were taken with a proton beam at 100 GeV and with electron beams at 11 different energies, ranging from 6 GeV to 250 GeV. Incidence angles were 0°, 4.5°, 7.5° and 15° [4].
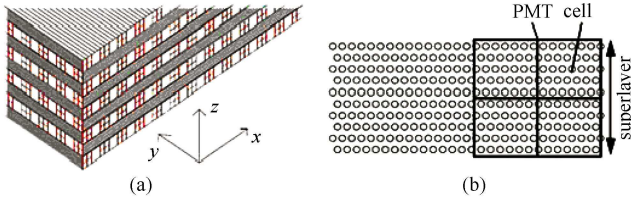

Fig. 1.   Structure of the AMS-02 ECAL. (a) The superlayer assembly; (b) the structure of a portion of a superlayer with one PMT.
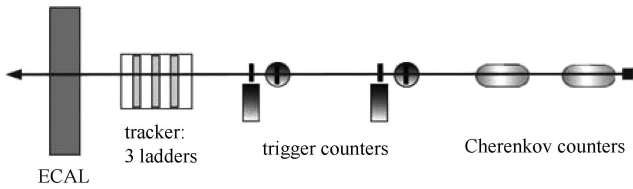

Fig. 2.   The AMS02 ECAL test beam setups.

3   Position reconstruction of one single layer

The most common method for single-layer position reconstruction is the Center of Gravity (COG) method, which takes the center of gravity of the deposited energy as the reconstructed position.   The Lateral Fit (LF) method can also be used for position reconstruction. This method uses the two dimensional lateral distribution of deposited energy in a single layer, as described by Eq. (1) [5]. The integral over a cell of the differential energy described by Eq. (1) is the theoretical value of energy deposited in the cell. Incidence position can be obtained by successfully fitting the theoretical value from measured energy using the Minuit package of ROOT software [6].

$$\frac{\mathrm{d}^2 E}{\mathrm{d}x\mathrm{d}y} = \frac{3 \cdot E_{\mathrm{Layer}}}{\pi} \cdot \frac{R_{\mathrm{Layer}}^2}{(r + R_{\mathrm{Layer}})^4}. \tag{1}$$

Although the LF method is more precise than the COG method, due to the complexity of the fit procedure and the limited granularity of the calorimeter, only about 60% of the events are fitted successfully with this method.   Eventually, none of these methods were satisfactory, so we decided to develop a new approach for the reconstruction of electromagnetic showers.

3.1   Neighbor cell deposited energy ratio (NCDER) method

When a high energy electron or photon hits the AMS-02 ECAL, there will be an electromagnetic shower in the ECAL. For a given layer, the cell through which the axis of the shower passes is defined as the central cell. Since the lateral distribution of electromagnetic showers is narrow, the central cell will be the one with most deposited energy.

The energy deposited in the right and left neighbors of the central cell is defined as E_{Right} and E_{Left}, respectively. For the AMS-02 ECAL test beam, the incidence position of the particle was obtained precisely from the track reconstruction in the silicon tracker ladders.

The ratio of E_{Left} to E_{Right} decreases exponentially with the distance of the incidence position to the left edge of the central cell, as shown in Fig. 3. Fig. 3 is elicited from 100 GeV electron events of AMS-02 test beam data. The dots in the plot represent results from events with 0° and 7.5° incidence angles, while the line represents the exponential fit curve. Events with 0° incidence angle are in perfect match with 7.5° events in Fig. 3, proving that the ratio does not depend on the incidence angle.
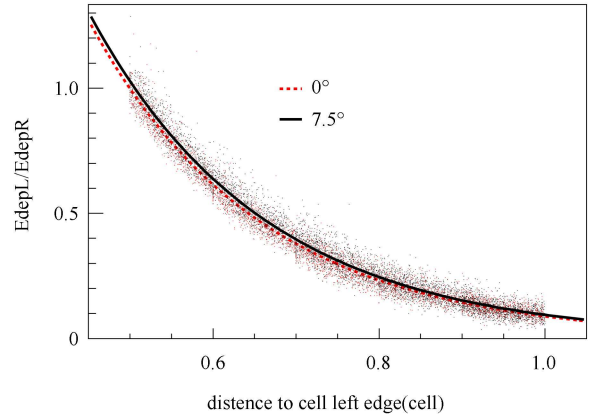

Fig. 3.   Deposited energy ratio of the left and right neighbor cells versus the distance from incidence position to the left edge of the cell.

The exponential function can be described by two parameters, as in Eq. (2):

$$\frac{E_{\mathrm{Left}}}{E_{\mathrm{Right}}} = \mathrm{e}^{A \cdot d + B}, \tag{2}$$

where d represents the distance from the incidence position to the left edge of the central cell. For electromagnetic showers: when a particle passes across the center

of the cell, the deposited energy in the left and right neighbor cells should be equal, thus:

$$\frac{E_{\text{Left}}}{E_{\text{Right}}} = e^{A \cdot d + B} = 1$$

$$\Rightarrow 0.5 \times A + B = 0$$

$$\Rightarrow B = -0.5 \times A.$$

So, Eq. (2) can be reduced to Eq. (3):

$$\frac{E_{\text{Left}}}{E_{\text{Right}}} = e^{\alpha \cdot d - 0.5 \cdot \alpha}. \quad (3)$$

The distance from the incidence position to the left edge of the cell is derived from Eq. (4).

$$d = 0.5 + \left(\ln\left(\frac{E_{\text{Left}}}{E_{\text{Right}}} \right) \right)/\alpha. \quad (4)$$

Thus, the incidence position $x_{\text{incidence}}$ is obtained from Eq. (5):

$$x_{\text{incidence}} = d + x_{\text{left\_edge}} = 0.5 + \ln\left(\frac{E_{\text{Left}}}{E_{\text{Right}}} \right)/\alpha + x_{\text{left\_edge}}. \quad (5)$$

$x_{\text{left\_edge}}$ in Eq. (5) represents the position of the left edge of the central cell, which can be obtained from the geometry specifications of the AMS-02 ECAL.

The value of α can be obtained layer by layer by fitting plots similar to Fig. 3, but for facility, the dependence of α value on layer number is studied with test beam data. Fig. 4, shows the plot of the value of α versus the layer number from the fourth layer onward for 100 GeV electrons. It is shown from the plot that the value of α decreases linearly with the layer number, starting from the fourth layer. The value of α can be described as Equation (6), where N_{layer} is the layer number, and $P1$ and $P2$ are parameters.

$$\alpha = P1 \cdot N_{\text{Layer}} + P2. \quad (6)$$

For the first four layers, the electromagnetic shower is not well developed, thus the weights for the final direction fitting [8] are very small. Consequently, Eq. (6) is used for deriving the value of α for the first three layers.

For 100 GeV electrons, with values of $P1$ and $P2$ taken from the fit in Fig. 4, α values for all layers can be derived from Eq. (6), then the incidence position $x_{\text{incidence}}$ for all layers can be obtained from Eq. (5).

For electrons with other energies, which were tested in the test beam, $P1$ and $P2$ can be obtained by a similar process. To make this method usable for all energies, $P1$ and $P2$ dependence on energy is studied with test beam data. $P1$ and $P2$ versus energy are shown in Fig. 5, where the stars represent the results obtained from test beam data, while the solid lines are fitting results with empirical functions.

For a real event, a preliminary value for the total energy can be reconstructed [7], then the value of $P1$ and $P2$ can be derived from the empirical functions obtained
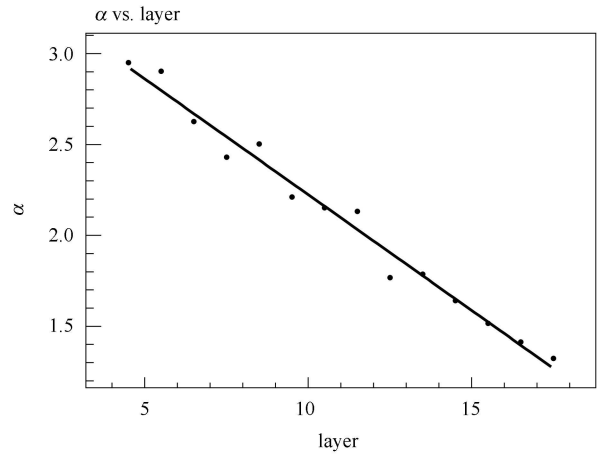

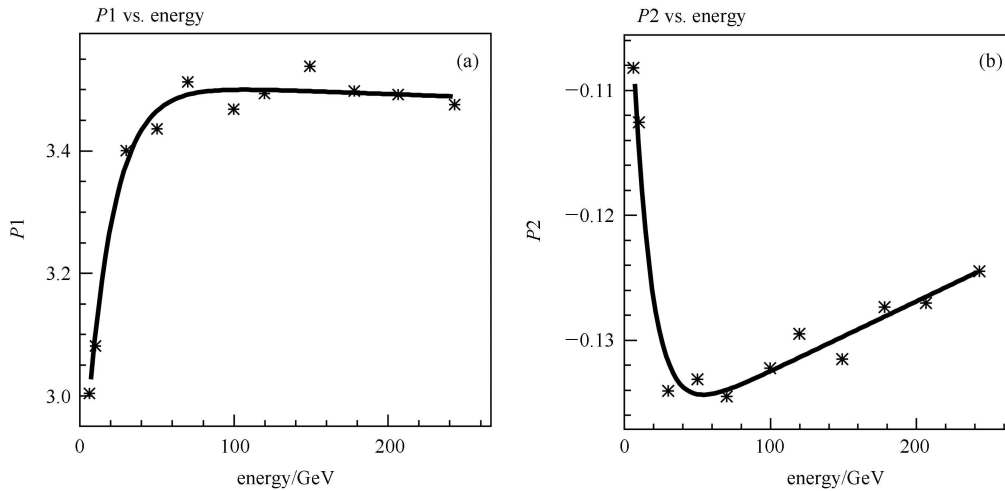Fig. 4. α value versus layer number.

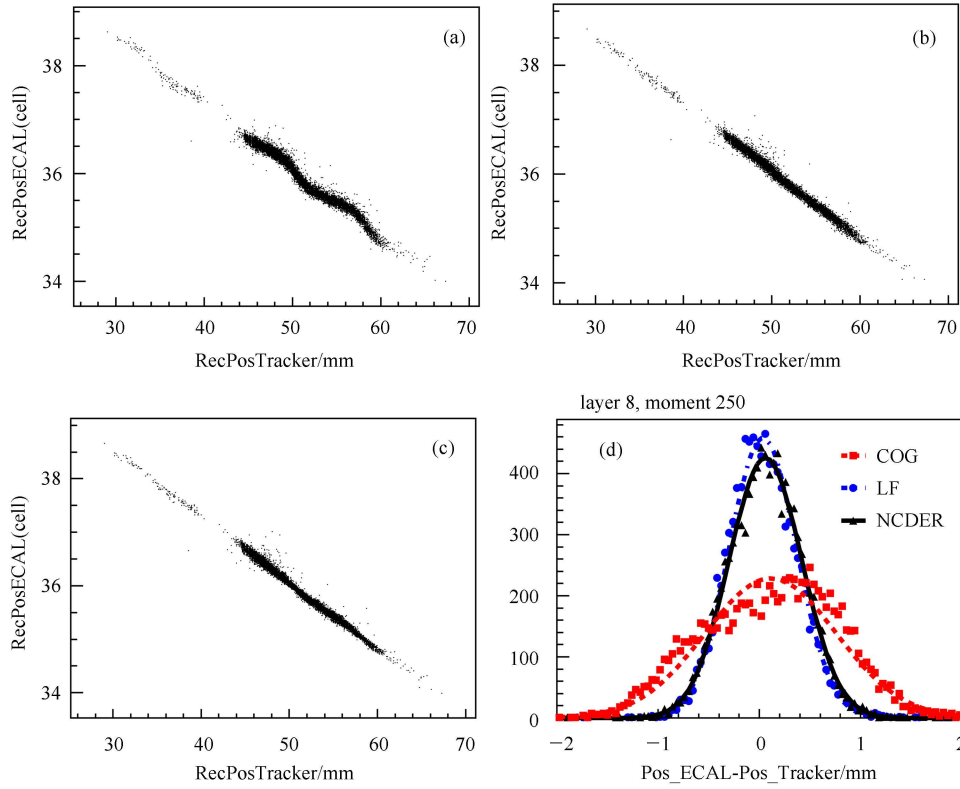Fig. 5.   (a) $P1$ versus energy; (b) $P2$ versus energy.

Fig. 6. Reconstructed positions in the eighth layer with (a) the COG method, (b) the NCDER method, (c) the LF method versus positions measured by the silicon trackers for 100 GeV electrons; (d) distribution of position₋ rec₋ ECAL - position₋ measure₋ Tracker for electrons of 250 GeV with 7.5° incidence angle, point line reconstructed using the COG methods, solid and dashed lines for the NCDER and LF methods, respectively.

from Fig. 5. Thus, α values for all layers can be obtained from Eq. (6), then the incidence position $x_{\text{incidence}}$ in all layers can be reconstructed from the α values and energy deposited in cells, using Eq. (5).

3.2   Comparison of the COG, LT and NCDER methods

A comparison between the incidence position evaluated in the ECAL, using the various reconstruction methods, and the position given by the silicon tracker for 100 GeV electrons, is shown in Fig. 6(a), (b) and (c). From these figures, it is evident that the reconstructed positions with LF and NCDER methods are linear with the position given by the silicon tracker, while that from the COG method is not - it tends to deviate towards the center of the cell.

The distribution of the differences between positions given by silicon trackers and positions reconstructed with these three methods, for 250 GeV electrons with 7.5° incidence angle, is plotted in Fig. 6(d), which shows that the results with NCDER and LF methods are clearly better than those from the COG method.

4   Reconstruction of incidence direction

The projection of incidence direction in the x-z plane, which is called K_x, can be obtained by weighted linear fitting of the reconstructed incidence positions in all 8 layers in the x view, and similarly for all 10 layers in the y view to obtain the projection in the y-z plane, K_y.

The distribution of K_x and K_y, fitted with positions reconstructed using the COG, NCDER and LF methods for 30 GeV electrons, is shown in Fig. 7. The beam incidence angles of electrons is 7.5° in the y-z projection and 0 in the x-z projection. From the plots, it is clear that the results given by the COG method have the worst resolution, and there is deviation in the K value for the results for inclined events.

The incidence angle can be calculated from K_x and K_y via the function: $\theta = \arctan\left(\sqrt{K_x^2 + K_y^2}\right)$ and $\Delta\theta = \arctan\left(\sqrt{(K_x - \overline{K_x})^2 + (K_y - \overline{K_y})^2}\right)$. If events with $\Delta\theta$ less than θ_{68} account for 68% of the total, then θ_{68} is defined as the angular resolution.
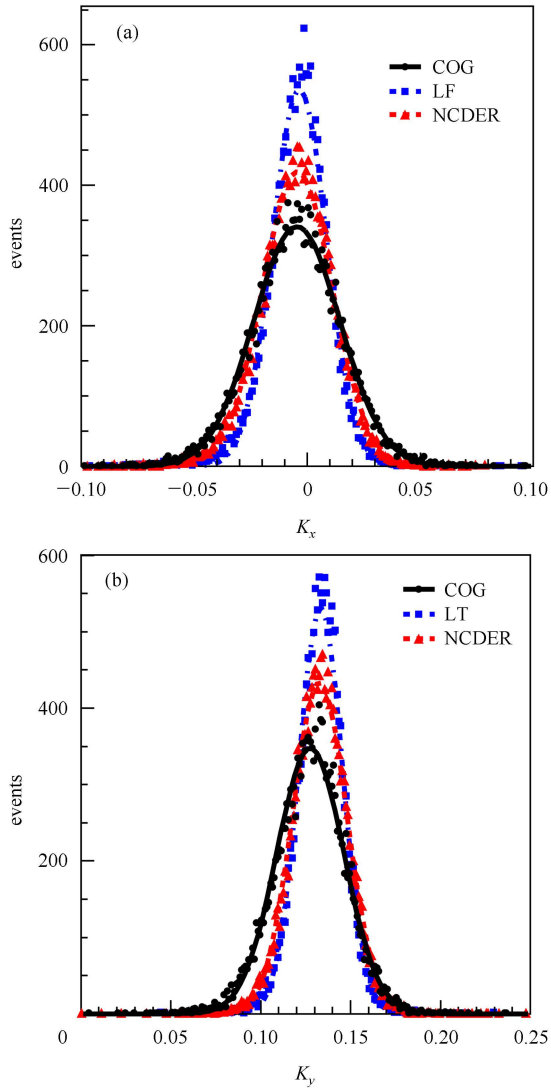
Fig. 7. K_x, K_y distribution. The circles with solid line are for the COG method, triangles with point-dash line are for the NCDER method, and squares with dashed line are for the LF method.

5   Results and conclusion

Perpendicular electron events with energies of 6, 10, 30, 50, 70, 100, 120, 150, 180, 200, and 250 GeV were reconstructed with the COF, LF and NCDER meth-

ods. Reconstruction with the NCDER method follows the process described above using the same set of parameters. Plots of angular resolution versus energy are shown in Fig. 8, which shows that angular resolution for results with the NCDER method and the LF method are much better than that from the COG method; for 100 GeV electrons, angular resolution improved from 1.10° to 0.79° and 0.63° respectively.
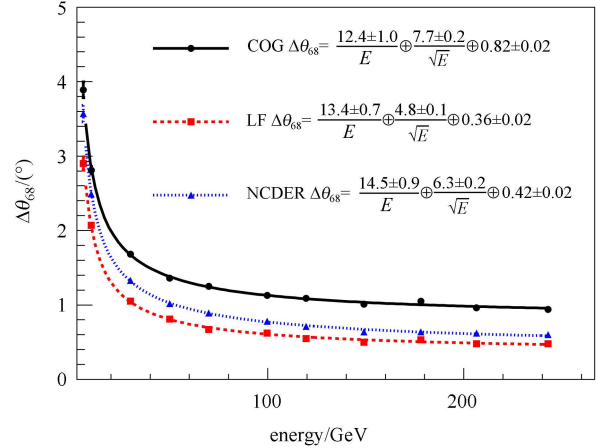

Fig. 8.   Angular resolution versus energy. The circles with solid line are for the COG method, triangles with point line are for the NCDER method, and squares with dashed line are for the LF method.

Electron events with energies of 10, 30, 100, 150, 250 GeV and 7.5° and 15° incidence angles were also reconstructed with the COF, LF and NCDER methods to check the reconstruction quality for inclined events. Reconstructed angles and angular resolutions with the three methods are listed in Table 1 and Table 2. Table 1 shows that incidence angles reconstructed using the COG method are clearly smaller for electrons with big angles, while ones reconstructed using the other two methods are equal to real values within the system error (the system error for the test beam is 0.2°; 0.1° for precision of rotating table and 0.1° for beam orientation.). Table 2 shows that angular resolutions change with the energy of the incidence particle, but remain the same for different incidence angles.

Table 1.   Reconstructed angles.

energy/GeV	10	10	30	30	100	100	100	150	150	250	250
$\theta_{\text{incidence}}/(°)$	7.5	15	7.5	15	4.5	7.5	15	7.5	15	7.5	15
$\theta_{\text{COG}}/(°)$	7.4	14.2	7.3	14.1	4.5	7.3	14.3	7.3	14.3	7.3	14.2
$\theta_{\text{NCDER}}/(°)$	7.7	14.8	7.6	14.8	4.7	7.6	14.8	7.6	14.9	7.5	14.8
$\theta_{\text{LF}}/(°)$	7.6	14.7	7.6	14.8	4.7	7.6	14.8	7.6	14.9	7.5	14.9

Table 2.   Angular resolution.

energy/GeV	10	10	30	30	100	100	100	150	150	250	250
$\theta_{\mathrm{incidence}}/(^\circ)$	7.5	15	7.5	15	4.5	7.5	15	7.5	15	7.5	15
$\theta_{68\mathrm{COG}}/(^\circ)$	2.82	2.95	1.64	1.70	1.09	1.04	1.10	1.02	1.04	0.93	0.84
$\theta_{68\mathrm{NCDER}}/(^\circ)$	2.55	2.72	1.33	1.36	0.80	0.74	0.76	0.68	0.74	0.58	0.58
$\theta_{68\mathrm{LF}}/(^\circ)$	2.10	2.24	1.05	1.10	0.63	0.59	0.62	0.54	0.59	0.48	0.46

In conclusion, the NCDER and LF methods are more accurate than the COG method for angular reconstruction. In addition, the reconstructed angle obtained using the COG method is smaller than the real value for inclined tracks, while there is no bias using the LF and NCDER methods. The angular resolution obtained using the LF method is about 20% better than the one obtained using the NCDER method, but the LF method needs a lot of CPU time and only 60% of the events can be successfully reconstructed. In comparison, with the NCDER method, almost 100% of the events are reconstructed, consuming barely any CPU time. A loss of 40% of the events means lower statistics for the experiment and this could generate a bias in results, which is not acceptable for an experiment like AMS. The optimal method for angular reconstruction is, therefore, the NCDER method.

References

1 Battiston R et al. Astropart. Phys., 2000, **13**: 51–74
2 Antonelli M et al. Nuclear Physics B, 1977, **54**: 14–19
3 Cadoux F et al. Nuclear Physics B, 2002, **113**(Proc.Suppl.): 159–165
4 Di Falco Stefano. Advances in Space Research, 2010, **45**(1): 112–122
5 TAO Jun-Quan et al. Chinese Physics C (HEP & NP), 2008, **32**(3): 191–195
6 http://www.root.cern.ch
7 LI Zu-Hao et al. HEP & NP, 2004, **28**: 1182-1188 (in Chinese)
8 WANG Xiao-Bin et al. HEP& NP, 2005, **29**: 1071 (in Chinese)